NANO LETTERS

2007
Vol. 7, No. 3
676−680

Single Wall Carbon Nanotube Scaffolds for Photoelectrochemical Solar Cells. Capture and Transport of Photogenerated Electrons

Anusorn Kongkanand, Rebeca Martínez Domínguez, and Prashant V. Kamat*

Radiation Laboratory, Departments of Chemistry & Biochemistry and Chemical & Biomolecular Engineering, University of Notre Dame, Notre Dame, Indiana 46556-0579

Received November 21, 2006; Revised Manuscript Received January 22, 2007

ABSTRACT

Single wall carbon nanotube (SWCNT) architecture when employed as conducting scaffolds in a TiO_2 semiconductor based photoelectrochemical cell can boost the photoconversion efficiency by a factor of 2. Titanium dioxide nanoparticles were dispersed on SWCNT films to improve photoinduced charge separation and transport of carriers to the collecting electrode surface. The shift of ~100 mV in apparent Fermi level of the SWCNT–TiO_2 system as compared to the unsupported TiO_2 system indicates the Fermi level equilibration between the two systems. The interplay between the TiO_2 and SWCNT of attaining charge equilibration is an important factor for improving photoelectrochemical performance of nanostructured semiconductor based solar cells. The feasibility of employing a SWCNT–TiO_2 composite to drive the water photoelectrolysis reaction has also been explored.

The photocatalytic activity of nanostructured semiconductor films has been widely explored in designing solar cells, solar hydrogen production, and environmental remediation.[1,2] Of particular interest is the dye-sensitized solar cell (DSSC) which uses mesoscopic (or nanostructured) TiO_2 films modified with sensitizing dyes. Despite the initial success of achieving 10% solar conversion efficiency, the effort to further improve their performance has not met with breakthroughs.[3,4] A major hurdle in attaining higher photoconversion efficiency in such nanostructured electrodes is the transport of electrons across the particle network. The photogenerated electrons in mesoscopic films for example have to travel through the network of semiconductor particles and encounter many grain boundaries during the transit. Such a random transit path for the photogenerated electrons increases the probability of their recombination with oxidized sensitizer.[5−7] The use of a redox couple such as I_3^-/I^- facilitates the electron transport to some extent by rapid regeneration of the oxidized sensitizer.

With the recent advance in the design of nanotube and nanowire architecture, it should be possible to use such one-dimensional nanostructures to direct the flow of photogenerated charge carriers.[8−10] The obvious challenge is to use nanowire or nanotube networks as support to anchor light-harvesting semiconductor particles and facilitate the electron transport to the collecting electrode surface in a solar cell. The scenarios that illustrate the electron transport in semiconductor particle based films and nanotube−nanoparticle composites are presented in Scheme 1.

The unique electrical and electronic properties, wide electrochemical stability window, and high surface area render single wall carbon nanotubes (SWCNTs) as scaffolds to anchor light-harvesting assemblies. The semiconducting SWCNTs have been shown to play an important role in improving the performance of organic photovoltaic cells[11] and fuel cells.[12,13] They also display photoelectrochemical effects under visible light irradiation.[14,15] TiO_2 and ZnO nanowires and nanotubes have also been employed in DSSC.[9,16−19] An effort was recently made to organize CdS quantum dots on SWCNTs.[20] Upon excitation of CdS nanoparticles, we were able to observe charge injection from excited CdS into SWCNTs. The electron-accepting ability of semiconducting SWCNTs thus offers an opportunity to facilitate electron transport and increase the photoconversion efficiency of nanostructure semiconductor based solar cells. Other semiconductor particles such as CdSe and CdTe when attached to carbon nanotubes can induce charge-transfer processes under visible light irradiation.[21−23] As shown previously, organization of photoactive donor acceptor assemblies (e.g., porphyrin and C_{60}) on electrode surfaces

* Author to whom correspondence should be addressed. E-mail: pkamat@nd.edu.

10.1021/nl0627238 CCC: $37.00
Published on Web 02/20/2007

Scheme 1. Electron Transport across Nanostructured Semiconductor Fims: (A) in the Absence and (B) in the Presence of a Nanotube Support Architecture

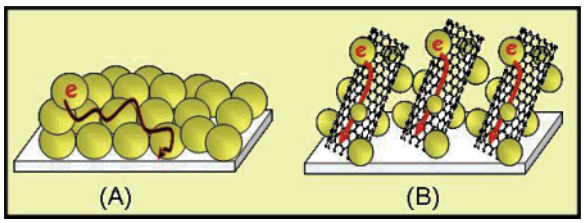

offers significant enhancement in the photoconversion efficiency of solar cells.[24−27]

We have successfully created SWCNT networks on a conducting carbon fiber and glass electrodes. The photoactive TiO_2 nanoparticles are then dispersed on a conducting scaffold of SWCNTs. The beneficial aspects of a SWCNT network in improving the photoelectrochemical performance are presented

Experimental Section. Electrode Preparation Cut pieces of carbon fiber paper (Toray paper, Fuelcellstore.com) and conducting glass were used to cast films of SWCNTs and TiO_2. SWCNTs purchased from SES Research were first refluxed in 5 M HNO_3 solution for 1 h to remove any metal and organic impurities and to open the end of the tubes by oxidation.[28−31] The sample was subjected to repeated cycles of washing and filtration to remove excess acid. The SWCNTs were solubilized in an organic solvent by sonication of dried SWCNTs in tetrahydrofuran (THF) containing (∼0.2 M) tetraoctylammonium bromide (TOAB). The detailed method can be found elsewhere.[32] The choice of a SES Research sample was based on the fuel cell performance comparison we made using several commercial samples.[12] The SWCNT sample that gave the superior performance was employed in the present photoelectrochemical studies.

SWCNTs were assembled as a thin film on a carbon fiber electrode (CFE) or optically transparent electrode (OTE) using an electrophoretic deposition technique.[32] A known amount of TOAB-solubilized SWCNT suspension in THF (0.2 mg/mL) was transferred to a 1 cm cuvette in which the CFE (or OTE) and a counter electrode (a conductive glass electrode) were kept at a distance of 4 mm. A dc voltage (60 V/cm) was applied between the electrodes using a Fluke 415 power supply. The deposition of the film can be visibly seen as the SWCNTs are driven to the electrode and the solution becomes colorless. These electrodes coated with SWCNT film are referred to as CFE/SWCNT and OTE/SWCNT, respectively.

The method employed to disperse TiO_2 particles on the carbon fiber paper was similar to the one described earlier.[33,34] TiO_2 powder (Degussa P-25 containing mostly in anatase form of TiO_2) was sonicated in 1% acetic acid methanol solution to obtain a 5 mg/mL TiO_2 suspension. The suspension was spread on the CFE and CFE/SWCNT electrodes by dropwise addition with the aid of a microsyringe. Drying under an air stream following each dropwise addition of TiO_2 suspension assisted quick evaporation of the solvent. This procedure continued until a desired amount

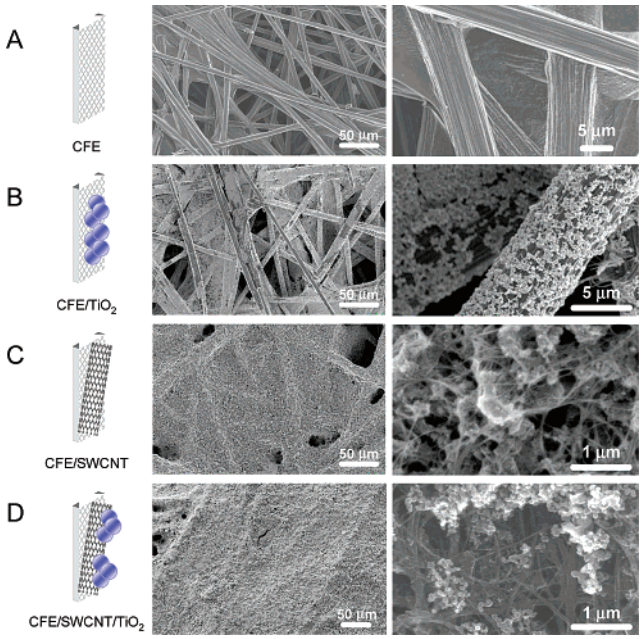

Figure 1. SEM of a carbon fiber electrode (CFE) at different stages of modification: (A) before surface modification; (B) after modification with TiO_2 particles; (C) after electrophoretic deposition of SWCNT; (D) after deposition of TiO_2 particles onto SWCNT film.

of TiO_2 was spread over CFE and CFE/SWCNT electrodes. The TiO_2 modified electrodes were then annealed at 473 K in air for 30 min. The same procedure was also followed to deposit TiO_2 on OTE/SWCNT electrodes. These electrodes coated with TiO_2 particles are referred as CFE/SWCNT/TiO_2 and OTE/SWCNT/TiO_2, respectively.

Photoelectrochemical Measurements. Half cell reactions were carried out in a conventional three-arm electrochemical cell using Pt foil as the counter electrode and a standard calomel electrode (SCE) as the reference electrode. Unless otherwise specified N_2-saturated 1 M KOH solution was used as an electrolyte. A 200 W Xe lamp (Oriel) with a copper sulfate filter (>300 nm) was employed as an excitation source. The intensity of the incident light near the electrode surface corresponded to 50 mW/cm^2. Photocurrent measurements were conducted using a 150 W Xe lamp equipped with quartz optics and monochromator to select the wavelength of excitation and using a Princeton Applied Research model PARSTAT 2263 potentiostat.

Results and Discussion. Modification of a Carbon Fiber Electrode (CFE) with SWCNTs and TiO_2. The carbon fiber paper is a popular choice to disperse catalyst particles in fuel cells since it facilitates the collection of electrons through carbon microfibers. In a previous study we described a hybrid fuel cell based on a photocatalyst and electrocatalyst deposited on a CFE.[34] We have now included a SWCNT architecture to disperse the TiO_2 particles with an aim to improve the photoconversion efficiency.

Figure 1 shows the low- and high-magnification scanning electron micrographs (SEM images) of carbon fiber paper (CFE) at different stages of modification. These images provide a perspective of the overall electrode morphology and the ability to anchor TiO_2 nanoparticles on CFE and

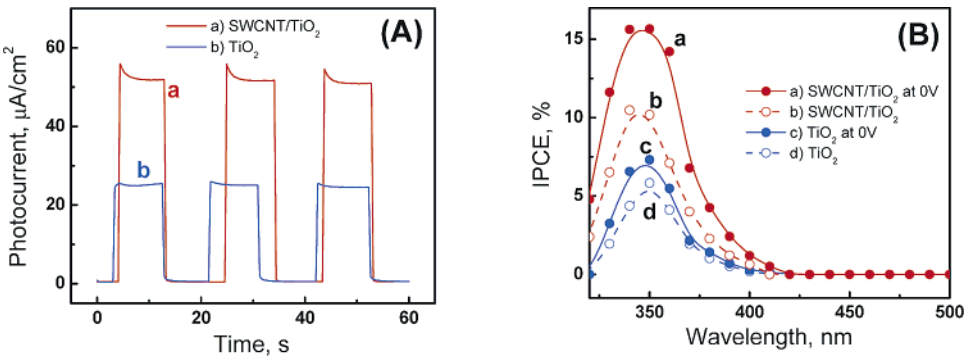

Figure 2. (A) Photocurrent response vs time profiles of CFE/SWCNT/TiO_2 (a) and CFE/TiO_2 (b) electrodes at 0 V vs SCE. Light intensity was 50 mW/cm^2 (λ > 300 nm). (B) Photocurrent action spectra of CFE/SWCNT/TiO_2 (a, b) and CFE/TiO_2 (c, d) electrodes at no applied bias (b, d) and at 0 V vs SCE (a, c). IPCE(%) = $(1240i_{sc})/(\lambda I_{inc}) \times 100$ where i_{sc} is short circuit current and I_{inc} is the power of the incident light. Electrolyte was N_2-saturated 1 M KOH solution.

SWCNT networks with a good dispersibility. The carbon fibers of the CFE electrode are in micrometer size (Figures 1A), and they serve as the backbone of the electrode in collecting photogenerated electrons and communicating with the external circuit. When TiO_2 particles are dispersed on the CFE, they get dispersed quite uniformly on carbon microfiber (Figure 1B). The higher magnification micrograph confirms the ability of carbon microfibers to support TiO_2 photocatalyst particles and collect photogenerated electrons.

In another set of experiments, SWCNTs were first deposited on to the carbon fiber electrode using an electrophoretic deposition method. This allowed us to extend the carbon support network at a nanometer scale. At low magnifications one can see the SWCNT film covering the void between the larger carbon microfiber network (Figure 1C). The magnified view of the same film shows a close interwoven network of SWCNT bundles. Such a support network of SWCNT has already been found useful in dispersing Pt and Pt−Ru electrocatalysts and improving the performance of hydrogen and methanol fuel cells.[35−37] The CFE/SWCNT was further modified by casting a film of TiO_2 nanoparticles. Figure 1D shows the micrograph of the electrode obtained after deposition of TiO_2 nanoparticles on the SWCNT network. In the high-magnification image we have deliberately selected an example that shows both TiO_2 particle aggregates and the underlying SWCNT network. Most of the other areas show complete coverage of TiO_2 particles. The aggregation of TiO_2 particles becomes predominant when we increase the ratio of [TiO_2]/[SWCNT]. If we keep the TiO_2 coverage sufficiently low, we can expect the SWCNT network to interact quite effectively with TiO_2 particles and facilitate charge transport in the composite film.

Photoelectrochemical Activity of Nanostructured TiO_2 Films. Films of TiO_2 particles undergo charge separation upon excitation with UV light (E_g > 3.2 eV). When employed as photoanodes in a photoelectrochemical cell, TiO_2 particulate films cast on electrode surface exhibit anodic photocurrent generation. The magnitude of the photocurrent represents the charge collection efficiency of the electrode surface. Figure 2A shows the short-circuit photocurrent generation at CFE/TiO_2 and CFE/SWCNT/TiO_2 electrodes. Both electrodes were prompt in generating photocurrent with a reproducible response to ON−OFF cycles. It is interesting to note that the TiO_2 particles deposited on a SWCNT network exhibited an enhanced photocurrent.

We further evaluated the electrode performance by recording the incident photon conversion to charge carrier conversion efficiency (IPCE) by monitoring the photocurrent at different incident wavelengths. The photocurrent action spectra of the two electrodes at short circuit and 0 V vs SCE are shown in Figure 2B. Both of these electrodes have a photocurrent onset at 380 nm corresponding to the band gap of TiO_2. In the absence of the SWCNT network we observe a maximum IPCE of 7.36% (350 nm) at 0 V vs SCE. The IPCE response shows a significant enhancement with an IPCE of 16% when a SWCNT scaffold supports the TiO_2 particles. Nearly doubling of the photoconversion efficiency is an indication of the improved charge collection efficiency using a SWCNT network.

Participation of a SWCNT Network in Photocurrent Enhancement. The commercial sample employed in the present study consists of nearly equal amounts of semiconducting and metallic carbon nanotubes. Our fuel cell experiments carried out with a Pt−SWCNT system shows that both semiconducting and metallic carbon nanotubes contribute toward improving the charge transfer and charge collection in both cathodic and anodic compartments. We expect a similar charge transport property of carbon nanotubes to improve the photocurrent generation.

In an earlier study[14] we have explored the photoelectrochemical properties of SWCNT films cast on electrode surfaces. The charge separation efficiency under visible excitation is quite low, and the observed photocurrent efficiency is quite low (<0.1%) as compared to the TiO_2 films. This low photoactivity rules out direct participation of SWCNT in the photocurrent generation. However, SWCNT support architecture is useful in enhancing the performance of electrocatalysts in fuel cells. For example, platinum nanoparticles dispersed on a SWCNT film show enhanced electrocatalytic activity in direct methanol fuel cells.[12] The SWCNT network was found to facilitate dispersion of the catalyst particles and decrease overall charge-transfer resistance for the electrode reaction.

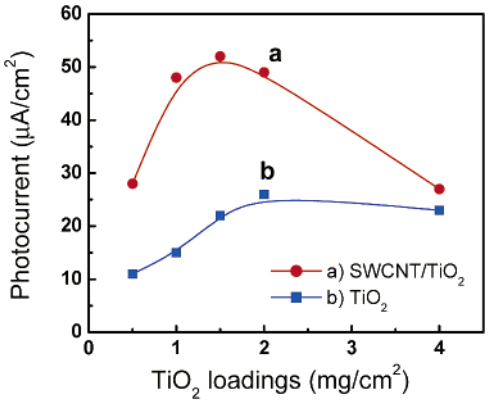

Figure 3. Photocurrent response as a function of the amount of TiO_2 deposited on CFE or CFE/SWCNT electrodes. Experimental conditions were the same as those in Figure 2A. SWCNT concentration was maintained constant at 0.2 mg/cm^2 while TiO_2 loading was varied.

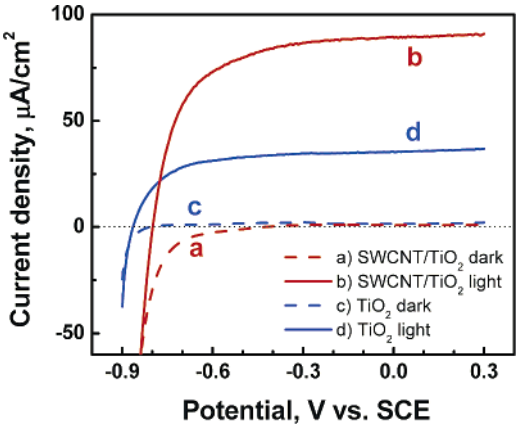

Figure 4. $I-V$ characteristics for OTE/TiO_2 (c, d) and OTE/SWCNT/TiO_2 (a, b) obtained with (b, d) and without (a, c) light illumination from the backside of the OTE. TiO_2 and SWCNT loadings were 2 and 0.01 mg/cm^2, respectively.

We probed the role of SWCNTs in enhancing the photoelectrochemical performance of TiO_2 film by varying the ratio of TiO_2/SWCNT in the composite film. The concentration of the SWCNTs was kept constant while TiO_2 loading was varied. Figure 3 compares the photocurrent observed with CFE/TiO_2 and CFE/SWCNT/TiO_2 electrodes at different loading of TiO_2 particles. In the case of CFE/TiO_2 film we observe an increase in photocurrent with increased TiO_2 loading (at loadings below 2 mg/cm^2) as more excited TiO_2 particles undergo charge separation and participate in the photocurrent generation. At higher TiO_2 loadings we observe saturation in the photocurrent showing the limitations of light absorption within the TiO_2 film. In the case of CFE/SWCNT/TiO_2 we observe a similar increasing trend at TiO_2 loadings up to 1.5 mg/cm^2. (Note that the CFE/SWCNT/TiO_2 electrodes were prepared with same amount of SWCNTs.) It is interesting to note that the photocurrent observed at these TiO_2 loadings is significantly greater than the photocurrent observed without the SWCNT support. This increase in the photoconversion efficiency parallels the experimental results discussed in Figure 2 and further supports our argument that the SWCNT support architecture plays an important role in improving the charge transport properties within the composite film. At these TiO_2 loadings, a SWCNT is capable of dispersing TiO_2 particles quite effectively and facilitate charge collection and transportation toward the collecting electrode surface. At higher loadings, however, we observe a decrease in the photocurrent as it approaches the value obtained in the absence of SWCNT. At these high TiO_2 loadings, the particles aggregate and most of these TiO_2 aggregates are not able to make a direct contact with the SWCNT bundles. The photoelectrochemical behavior at high TiO_2 loadings (4 mg/cm^2) thus tends to be similar for both CFE/TiO_2 and CFE/SWCNT/TiO_2. These experiments thus demonstrate the usefulness of SWCNT support architecture in improving the photocurrent generation in TiO_2-based photoelectrochemical solar cells.

Charge Equilibration. In order to probe the charge transfer interactions between the excited TiO_2 particles and SWCNT, we analyzed the current−voltage ($I-V$) characteristics of the OTE/TiO_2 and OTE/SWCNT/TiO_2 electrodes. The films deposited on optically transparent electrodes (OTEs) provided responses similar to those obtained with CFEs. Casting of films on OTEs allowed us to anneal the TiO_2 films at higher temperature (673 K) and obtain better electrochemical performance compared to CFE-based electrodes. The $I-V$ characteristics of TiO_2 and SWCNT−TiO_2 films in 1 M KOH solution recorded using dark and UV illumination are shown in Figure 4.

As shown earlier, the application of anodic bias facilitates charge separation in TiO_2 particulate films. The anodic bias provides the necessary driving force for transport of electrons to the collecting electrode surface and thus minimizes charge recombination. Both OTE/TiO_2 and OTE/SWCNT/TiO_2 exhibit similar enhanced photocurrent response at positive applied potentials. The OTE/SWCNT/TiO_2 exhibits higher photocurrent than OTE/TiO_2, thus confirming the role of conducting SWCNT scaffold in improving the overall photoelectrochemical performance. However, the potentials corresponding to zero current (often referred as flat band potential) are different. The flat band potentials as recorded from the zero current potential (Figure 4) were −0.86 and −0.79 V vs SCE for TiO_2 and SWCNT−TiO_2 films, respectively. Such a positive shift in the flat band potential is an indication of the electron transfer from TiO_2 to SWCNT as the two systems undergo charge equilibration. Since the conduction band of SWCNT (∼0 V vs NHE) is expected to be lower than that of TiO_2 (−0.5 V vs NHE), we expect charge equilibration between the two systems causing the shift of apparent Fermi level to more positive potentials. The shift of ∼70 mV in apparent Fermi level of the SWCNT−TiO_2 system is a further indication that the interplay between the two systems in charge equilibration is an important factor in controlling its photoelectrochemical properties.

Since the photogenerated holes reaching the electrode surface participate in the water oxidation reaction, one can evaluate the photoconversion efficiency (η) for water splitting reaction based on the expression (1)[38]

$$\eta = \text{power output/Incident power} = V_{WS} \times I_{sc}/I_{inc} \quad (1)$$

where V_{WS} refers to thermodynamic voltage for water-splitting reaction, I_{sc} refers to short circuit current, and I_{inc} is the incident light intensity (50 mW/cm^2). If one assumes the electrolysis efficiency proceeds with 100% water splitting reaction, one can use V_{WS} as 1.23 V (the ideal chemical energy limit at 297 K). Using the current value of 36 and 81 μA/cm^2 (obtained independently under no bias conditions), we obtain an efficiency of 0.09 and 0.20% for OTE/TiO_2 and OTE/SWCNT/TiO_2 electrodes (0.06 and 0.12% for CFE/TiO_2 and CFE/SWCNT/TiO_2). (*It should be noted that some of the high efficiency values reported in the literature makes use of the current values obtained under potentiostat bias conditions. The additional power extracted from the potentiostat to maintain the electrode at a set potential is difficult to estimate accurately. Hence caution should be exercised while comparing such high efficiency values.*)[39−41] Nevertheless, the observed values in the present study are at least an order of magnitude lower than those recently reported for TiO_2 nanotube and nanorod nanostructure films.[19,42] The anatase TiO_2 (P25) employed in this study is known to be inferior to the rutile TiO_2 for solar hydrogen production. The efficiency evaluation is made to demonstrate the usefulness of SWCNT in improving the poor performance of photocatalysts. Efforts are underway to employ rutile TiO_2 nanoparticles and further improve the efficiency of the photocatalytic process.

The SWCNT architecture provides a nanowire network to disperse TiO_2 particles. An increase of photoconversion efficiency (IPCE) represents the beneficial role of the SWCNT as conducting scaffold to facilitate charge collection and charge transport in nanostructured semiconductor films. Such nanowire/nanoparticle architecture is likely to play an important role in improving the efficiency of nanostructure-based solar cells, e.g., dye-sensitized solar cells or in water photoelectrolysis.

Acknowledgment. The research described herein was supported by the Office of Basic Energy Science of the Department of the Energy. R.M.D. acknowledge the support of the National Science Foundation for providing support under the Notre Dame Nano-Bio REU program. We also acknowledge the support of Professor Istvan Barsony, Research Institute for Technical Physics and Materials Science of the Hungarian Academy of Sciences, Budapest, for hosting the REU students and the assistance in recording the scanning electron microscopy images. We also thank Professors Vinodgopal, Istvan Robel, and Brian Seger for helpful discussions. This is contribution NDRL-4698 from the Notre Dame Radiation Laboratory.

References

(1) (a) Kamat, P. V. *Chem. Rev.* **1993**, *93*, 267. (b) Kamat, P. V. *J. Phys. Chem. C* **2007**, *111*, 2834.
(2) Bard, A. J.; Fox, M. A. *Acc. Chem. Res.* **1995**, *28*, 141.
(3) Meyer, G. J. *Inorg. Chem.* **2005**, *44*, 6852.
(4) Gratzel, M. *Inorg. Chem.* **2005**, *44*, 6841.
(5) Gratzel, M. *J. Photochem. Photobiol., A* **2004**, *164*, 3.
(6) Heimer, T. A.; Heilweil, E. J.; Bignozzi, C. A.; Meyer, G. J. *J. Phys. Chem. A* **2000**, *104*, 4256.
(7) Kamat, P. V.; Haria, M.; Hotchandani, S. *J. Phys. Chem. B* **2004**, *108*, 5166.
(8) Sirbuly, D. J.; Law, M.; Yan, H.; Yang, P. *J Phys. Chem. B* **2005**, *109*, 15190.
(9) Law, M.; Greene, L. E.; Johnson, J. C.; Saykally, R.; Yang, P. *Nat. Mater.* **2005**, *4*, 455.
(10) Klimov, V. I. *J. Phys. Chem. B* **2006**, *110*, 16827.
(11) Hoppe, H.; Sariciftci, N. S. *J. Mater. Res.* **2004**, *19*, 1924.
(12) Girishkumar, G.; Hall, T. D.; Vinodgopal, K.; Kamat, P. V. *J. Phys. Chem. B* **2006**, *110*, 107.
(13) Kongkanand, A.; Vinodgopal, K.; Kuwabata, S.; Kamat, P. V. *J. Phys. Chem. B* **2006**, *110*, 16185.
(14) Barazzouk, S.; Hotchandani, S.; Vinodgopal, K.; Kamat, P. V. *J. Phys. Chem. B* **2004**, *108*, 17015.
(15) Hasobe, T.; Fukuzumi, S.; Kamat, P. V. *Angew. Chem., Int. Ed.* **2006**, *45*, 755.
(16) Adachi, M.; Murata, Y.; Okada, I.; Yoshikawa, S. *J. Electrochem. Soc.* **2003**, *150*, G488.
(17) Galoppini, E.; Rochford, J.; Chen, H.; Saraf, G.; Lu, Y.; Hagfeldt, A.; Boschloo, G. *J. Phys. Chem. B* **2006**, 16159.
(18) Mor, G. K.; Shankar, K.; Paulose, M.; Varghese, O. K.; Grimes, C. A. *Nano Lett.* **2006**, *6*, 215.
(19) Mor, G. K.; Shankar, K.; Paulose, M.; Varghese, O. K.; Grimes, C. A. *Nano Lett.* **2005**, *5*, 191.
(20) Robel, I.; Bunker, B.; Kamat, P. V. *Adv. Mater.* **2005**, *17*, 2458.
(21) Olek, M.; Busgen, T.; Hilgendorff, M.; Giersig, M. *J. Phys. Chem. B* **2006**, *110*, 12901.
(22) Ravindran, S.; Chaudhary, S.; Colburn, B.; Ozkan, M.; Ozkan, C. S. *Nano Lett.* **2003**, *3*, 447.
(23) Guldi, D. M.; Rahman, G. M. A.; Sgobba, V.; Kotov, N. A.; Bonifazi, D.; Prato, M. *J. Am. Chem. Soc.* **2006**, *128*, 2315.
(24) Hasobe, T.; Imahori, H.; Kamat, P. V.; Fukuzumi, S. *J. Am. Chem. Soc.* **2005**, *127*, 1216.
(25) Hasobe, T.; Kamat, P. V.; Troiani, V.; Solladie, N.; Ahn, T. K.; Kim, S. K.; Kim, D.; Kongkanand, A.; Kuwabata, S.; Fukuzumi, S. *J. Phys. Chem. B* **2005**, *109*, 19.
(26) Hasobe, T.; Fukuzumi, S.; Kamat, P. V. *J. Am. Chem. Soc.* **2005**, *127*, 11884.
(27) Hasobe, T.; Fukuzumi, S.; Kamat, P. V. *J. Phys. Chem. B* **2006**, *110*, 25477.
(28) Liu, J.; Rinzler, A. G.; Dai, H. J.; Hafner, J. H.; Bradley, R. K.; Boul, P. J.; Lu, A.; Iverson, T.; Shelimov, K.; Huffman, C. B.; Rodriguez-Macias, F.; Shon, Y. S.; Lee, T. R.; Colbert, D. T.; Smalley, R. E. *Science* **1998**, *280*, 1253.
(29) Liu, J.; Casavant, M. J.; Cox, M.; Walters, D. A.; Boul, P.; Lu, W.; Rimberg, A. J.; Smith, K. A.; Colbert, D. T.; Smalley, R. E. *Chem. Phys. Lett.* **1999**, *303*, 125.
(30) Chen, J.; Rao, A. M.; Lyuksyutov, S.; Itkis, M. E.; Hamon, M. A.; Hu, H.; Cohn, R. W.; Eklund, P. C.; Colbert, D. T.; Smalley, R. E.; Haddon, R. C. *J. Phys. Chem. B* **2001**, *105*, 2525.
(31) Mamedov, A. A.; Kotov, N. A.; Prato, M.; Guldi, D. M.; Wicksted, J. P.; Hirsch, A. *Nat. Mater.* **2002**, *1*, 190.
(32) Kamat, P. V.; Thomas, K. G.; Barazzouk, S.; Girishkumar, G.; Vinodgopal, K.; Meisel, D. *J. Am. Chem. Soc.* **2004**, *126*, 10757.
(33) Vinodgopal, K.; Hotchandani, S.; Kamat, P. V. *J. Phys. Chem.* **1993**, *97*, 9040.
(34) Drew, K.; Girishkumar, G.; Vinodgopal, K.; Kamat, P. V. *J. Phys. Chem. B* **2005**, *109*, 11851.
(35) Sun, X.; Li, R.; Villers, D.; Dodelet, J. P.; Desilets, S. *Chem. Phys. Lett.* **2003**, *379*, 99.
(36) Girishkumar, G.; Vinodgopal, K.; Meisel, D.; Kamat, P. V. *J. Phys. Chem. B* **2004**, *108*, 19960.
(37) Girishkumar, G.; Rettker, M.; Underhile, R.; Binz, D.; Vinodgopal, K.; McGinn, P.; Kamat, P. *Langmuir* **2005**, *21*, 8487.
(38) Khaselev, O.; Turner, J. A. *Science* **1998**, *280*, 425.
(39) Fujishima, A. *Science* **2003**, *301*, 1673a.
(40) Haegglund, C.; Graetzel, M.; Kasemo, B. *Science* **2003**, *301*, 1673b.
(41) Lackner, K. S. *Science* **2003**, *301*, 1673c.
(42) Paulose, M.; Shankar, K.; Yoriya, S.; Prakasam, H. E.; Varghese, O. K.; Mor, G. K.; Latempa, T. A.; Fitzgerald, A.; Grimes, C. A. *J. Phys. Chem. B* **2006**, *110*, 16179.

NL0627238